Journal of Neonatal Surgery
ISSN(Online): 2226-0439
Vol. 14, Issue 32s (2025)
https://www.jneonatalsurg.com

OPEN ACCESS

Development and Assessment of Copper Nanoparticles Synthesized from *Wild carrot.* Leaf Extract for Cancer Therapy

Rimmy Nandal[1], Amit Attri[1], Priya Dhiman[2], Varsha Rathee[1], Vikash Khandodiya[1], Vinay Nain[1], Yogesh Kinha[1], Sachin Saharan[1], Pooja Rani[*3]

[1]Shri Baba Mastnath Institute of Pharmaceutical Sciences and Research, Baba Mastnath University, Rohtak-124021

[2]SRM Modinagar College of Pharmacy, Faculty of Medicine and Health Sciences, SRM Institute of Science and Technology, Delhi-NCR Campus, Ghaziabad (Uttar Pradesh, India

[3]Chandigarh Group of Colleges Jhajeri, Mohali, Chandigarh Pharmacy College-Jhanjeri, Mohali (Punjab), India, 140307

Corresponding Author:

Dr. Pooja Rani*

Chandigarh Group of Colleges Jhajeri, Mohali, Chandigarh Pharmacy College-Jhanjeri, Mohali (Punjab), India, 140307

Cite this paper as: Rimmy Nandal, Amit Attri, Priya Dhiman, Varsha Rathee, Vikash Khandodiya, Vinay Nain, Yogesh Kinha, Sachin Saharan, Pooja Rani, (2025) Development and Assessment of Copper Nanoparticles Synthesized from Wild carrot. Leaf Extract for Cancer Therapy. *Journal of Neonatal Surgery*, 14 (32s), 1530-1540.

ABSTRACT

All over the world, Cancer is the most fatal disease. Various forms of cancer can be treated with a variety of medication groups. The leaves extract of *Wild carrot* was used in this study to formulate Copper nanoparticles utilizing a Green synthetic method. NPS were successfully synthesized using the Copper Sulphate Solution as the precursor of copper and leaf extract *Wild carrot* of the 50 ml (5 mm) of $CuSO_4$ was stimulated to react using the plant extracts. The nanoparticles exhibited a cuboidal shape and had an average size of 36.7nm, 53.5nm and 75.6 nm. FTIR spectrum analysis shows absorption peak of copper nanoparticles bonding among 1509-3917cm^{-1}. In the SEM, the particle shape was found to be Cuboidal. The results showed that the copper nanoparticles demonstrated significant anticancer potential with a GI_{50} value of >80ug/ml of plant and copper nanoparticles. As compare to standard drug with a GI_{50} value of <10ug/ml a strong inhibitory effect on the cancer cells.

Keywords: *Copper nanoparticles, leaf extract, Wild carrot, Cancer*

1. INTRODUCTION

We can see cancer treatment modalities by dividing them into conventional (traditional) and advanced or novel or modern categories. In this era worldwide, over half of all ongoing medical treatment trials are focusing on cancer treatments. Entities, such as the type of cancer, its site, and severity, guide to select treatment options and its progress. The most widely used traditional treatment methods are surgery, chemotherapy, and radiotherapy, while modern modalities include hormone therapy, anti-angiogenic, stem cell therapies, immunotherapy, and dendritic cell-based immunotherapy (Debela et al., 2021).

The largest obstacles to treating cancer and lessening its symptoms are drug resistance and its delivery systems, despite the fact that there are currently a number of approved therapy modalities and drugs. Traditional cancer treatment is no longer as successful as it once was because of abnormal blood vessel architecture and tumour biology. The most cutting-edge and creative cancer therapeutic approaches are listed below, along with their advantages and disadvantages. Other methods, including targeted therapy, nanomedicine, gene therapy, siRNA shipment, immunization and molecules of antioxidants enhance the bio-distribution of newly created or tested chemotherapeutic agents around the particular tissue that needs to be treated (Dashtizadeh. *et al*., 2021; Kumari *et al*., 2024).

A variety of copper NPs can be produced utilizing physically and chemically method. The disadvantages of these physical or chemical methods for producing copper nanoparticles include the expensive cost of the chemicals employed, the creation of dangerously hazardous compounds, and the time-consuming process for isolating the nanoparticles (Thakur et al., 2014). The biomedical sciences have made substantial use of copper nanoparticles made through green synthesis using medicinal plants to treat a variety of diseases. The primary therapeutic features of copper nanoparticles generated by plants are

anticancer effects (Liu et al.,2021; Kumari et al., 2025). Copper nanoparticles derived from plant extracts have greater potential applications as antibacterial agents since copper is less expensive than silver. For topically applied applications, a copper nanomaterial with photochemical encapsulation is advantageous (Tahvilian et al., 2019). In instance, fungal diseases like candidiasis may respond favourably to the synthetic copper nanoparticles as a treatment for a variety of bacterial ailments. The copper nanoparticles that were created are encapsulated, making them appropriate for use as antibacterial agents in topical medications. Additionally, the described green synthesis technique has significant therapeutic promise because it produces nanoparticles that are photochemical/ poly phenol - encapsulated. This contrasts with the charred nanoparticles that are created using conventional thermal-chemical techniques (Das et al., 2022)

2. MATERIAL AND METHOD

Wild carrot leaves are collected from Hisar (Haryana). Firstly leaves were washed with tap H_2O and then washed with deionized H_2O. Dried leaves was grinder by using motar pestle. 25 gm of grinding of leaves material added into the 250 ml ethanol extracting using soxhlet method. After, the extraction, then it filtered using what filter paper no. 1 and stored in a room temperature (Anaja et al., 2016).5 ml of an aqueous plant extract were mixed with 50 ml of a copper sulphate pentahydarte solution (5 mM). For later use, a dark green powder that was obtained was kept at temperature. Centrifugation was used to separate the synthesized copper nanoparticles for 10 min. at 6,000 rpm. After the mixture was centrifuged, pellets were collected, and they were overnight dried at 60°C in a hot air oven. Copper nanoparticle was formulated by green synthesis method. Phytochemical analysis was performed for the following components such as alkaloids, amino acids, carbohydrates, phenolic compounds, saponins, flavanoids, and terpenoids (Sundaram et al., 2020; Verma et al., 2016).

3. EVALUATION OF COPPER NANOPARTICLES:

3.1 UV-Visible spectroscopy:

Double beam UV-VIS spectroscopy was used to optically measure the synthesized copper nanoparticles. It makes use of visible range absorption spectroscopy and right away changes the color of the substances in the area. Quantitative measurements of different ions, compounds, and biological macromolecules at different wavelengths make up the majority of its analytical chemistry applications. Various wavelengths between 250 and 350 nm were used to examine the synthesized CuNPs' optical characteristics (Mali et al., 2020; Rani et al., 2024).

3.2 Scanning Electron Microscope:

The sample, needed uncertainty, and SEM performance all influence the size of nanoobjects that can be quantified accurately. STEM detectors are a regular feature of modern SEMs; however, STEM signals can also be detected using specialized sample holders, as illustrated in A thin coating of gold transforms some of the primary electrons into transmitted electrons (TE), which are then transformed into secondary electrons. The standard Everhart-Thornley (E-T) detector then picks up these SEs as a transmitted electron signal. By using electric fields or simple shielding, other SEs can avoid detection (Devi et al., 2020; Sarkar et al., 2017).

3.3 X Ray Diffraction:

X-ray diffractometers are used in XRD to identify the crystalline structure of materials. An X-ray powder XRD pattern is produced by the parallel X-ray beam that the XRD equipment produces and directs onto a sample of crystals. It is possible to determine the atomic orientation of NPs and, consequently, their crystal structure, using this powder XRD pattern. To ensure proper instrumentation and analysis are employed with this technique, it is crucial to have some knowledge about the crystal's elemental composition and standards (Rani et al., 2024).

3.4 Fourier transforms infrared spectroscopy:

When identifying organic materials like polymers and polymer compounds, Fourier transform infrared spectroscopy is used. This method reveals how infrared light influences the rotation and vibration of molecules. FTIR analysis has been used to characterise bacteria exposed to nanoparticles and can be performed on both solid and liquid samples. FTIR makes it simple to identify the characteristics of the functional groups and metabolites that are found on the surface of nanoparticles, and this occasionally aids in the stabilisation and reduction of nanoparticles (Valsalam et al., 2018).

3.5 Gas Chromatography Mass Spectroscopy (GCMS):

The GC–MS technique was adopted for the detection and identification of phytochemical compounds present in copper nanoparticles of spices. It was carried out using a PerkinElmer GC Clarus 500 system (Waltham, MA, USA). The GC–MS detection was executed using electron impact mode with an ionization energy of 70 eV. The carrier gas was helium (99.999%) with a constant flow rate of 1 mL/min and the injection volume was 1 µL. Temperature settings were: injector temperature, 250°C; ion-source temperature, 200°C; and oven temperature, 110–280°C (13).

3.6 Anticancer Activity (SBR Assay):

In this study, cell lines were cultured in a medium supplemented with 10% fetal bovine serum and 2 mM glutamine. For the screening test, 5000 cells were added per well in 96-well microtiter plates and incubated for 24 hours. Experimental drugs were prepared by diluting frozen stocks with water to obtain concentrations of 10 µg/ml, 20 µg/ml, 40 µg/ml, and 80 µg/ml. Following a 48-hour incubation with the drugs, the test was halted using cold trichloroacetic acid (TCA). Fixed cells were then treated with 0.4% sulforhodamine B (SRB) solution in 1% acetic acid, and after 20 minutes, the plates were washed, dried, and dye was eluted with 10 mM trizma base. Absorbance was measured at 540 nm with a reference wavelength at 690 nm. The percentage growth was computed by comparing test wells against control wells. The concentration causing a 50% reduction in net protein increase was deemed the GI_{50}. Values for GI_{50}, TGI, and LC_{50} were determined if desired activity levels were attained; otherwise, outcomes were indicated as exceeding or falling below the tested concentration range.

4. RESULT AND DISCUSSION

4.1 UV-Visible Spectroscopy (Calibration Curve):

By scanning the produced solution in the 250-300 nm wavelength range, the maximum concentration of the λ_{max}*Wild carrot* drug was identified. It was discovered that the maximum wavelength was 280 nm. *Wild carrot* calibration at pH 8-9. Using concentration range of 2–10 µg/ml the curve was prepared and is found to be linear and the regression coefficient (R^2) is 0.9997.

Concentration (µg/mL)	Absorbance value
0	0
2	0.039
4	0.082
6	0.121
8	0.159
10	0.201

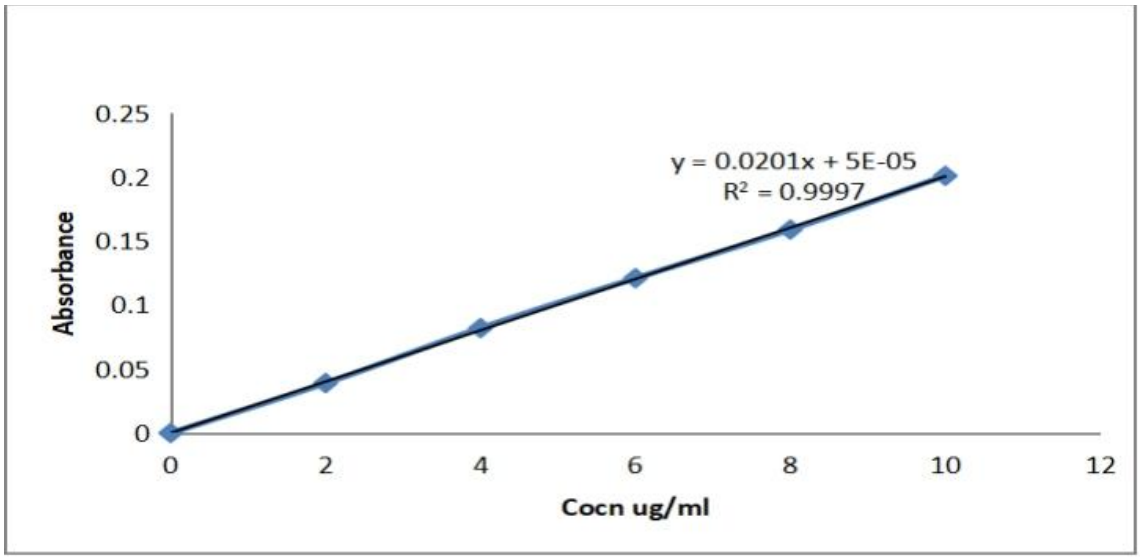

Fig.1: Calibartion curve of Wild carrot

4.2 SCANNING ELECTRON MICROSCOPY:

Scanning Analysis of the particle morphology was done using scanning electron microscopy. The nanoparticles were spherical-shaped, as was evident from the SEM picture. The variability grades of the copper - (II) as a precursor, which are

a natural component, may result in products with varying morphologies. Copper nanoparticles show the highest absorption peaks value. The images were estimated 200 nanoscale magnitudes which clearly show in this picture.

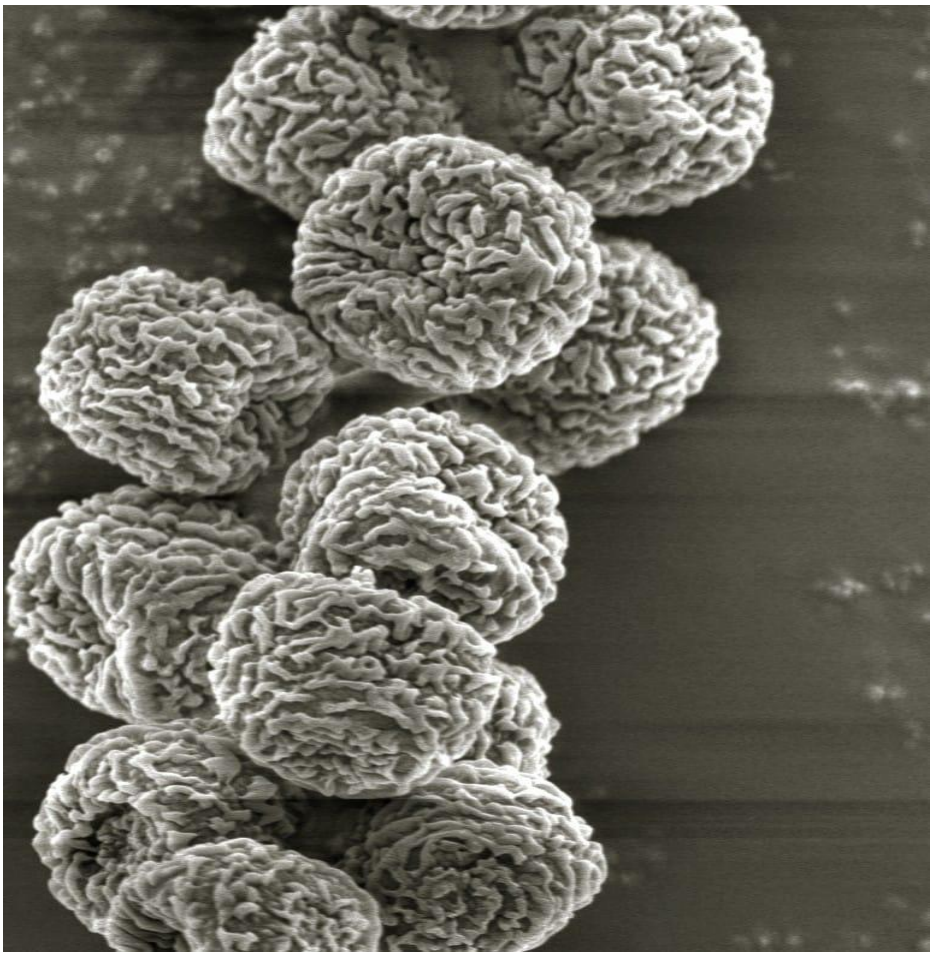

Fig.2: SCANNING ELECTRON MICROSCOPY

4.3 XRD ANALYSIS:

The Rigaku Miniflex-600 diffractometer model was used for the XRD analysis. At room temperature, a Cu K source operation (40 kV, 15 mA) was used. The size of the nanoparticles was calculated using Scherer's equation. X is the X average crystal size, K is the Scherer coefficient (0.89), is the Bragg's angle (2θ)total width at half maximum in degrees. The (111), (200), and (220) set of lattice planes are the ones that correspond to the various Bragg's reflections that copper displays. We can conclude that synthetic copper nanoparticles are face-centered cubic and fundamentally crystalline in nature based on these Bragg reflections. The set of lattice planes (111), (200), and (220) were found to be extremely weak and widened relative to each other. This characteristic shows that biologically nanocrystals are highly anisotropic and that the nanoparticles are (111) orientated, according to Bragg's reflection (111).

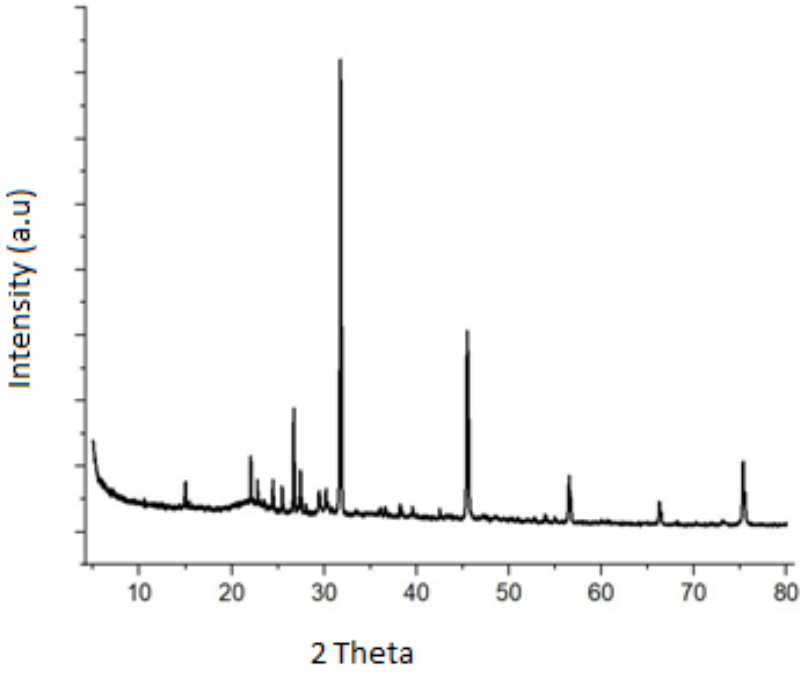

Fig. 3 :X-ray diffraction spectrum of Copper nanoparticle

4.4 FTIR ANALYSIS:

FTIR analysis was conducted in this study to identify the biomolecules present on the surface of the synthesized copper nanoparticles, responsible for their reduction. the nanoparticles showed several distinctive peaks, as depicted in Figure. These peaks were observed in the region of 1509-3917 cm-1. The absorption peak at 1509 cm-1 can be attributed to the presence of aromatic -C=C bonds. Peaks around 1608 cm-1 are associated with alkene C=C bonds, while the peak at 1713 cm-1 is likely due to carbonyl groups of -C=O. The peak observed at 3010 cm-1 may be attributed to aromatic C-H bonds. Additionally, the peak at 3648 cm-1 is likely due to the presence of alcohol -O-H functional groups. These results strongly support the hypothesis that the water-soluble heterocyclic components present in the leaf extract of *Wild carrot*, such as flavones, Iso-flavones, flavonols, neoflavonols, alkaloids, Coumarins, and anthocyanes, are responsible for reducing and capping the copper nanoparticles. The presence of oxygen atoms may also play a role in facilitating the absorption of these heterocyclic components on the surface of the copper nanoparticles and stabilizing them. The changes in peak amplitudes and slight shifts observed in the spectra can be attributed to the different capping species and the nature of coordination with the metal surface of the copper nanoparticles. Overall, the FTIR analysis gave important new information about the biomolecules in charge of the stabilization and reduction of the synthesised copper nanoparticles.

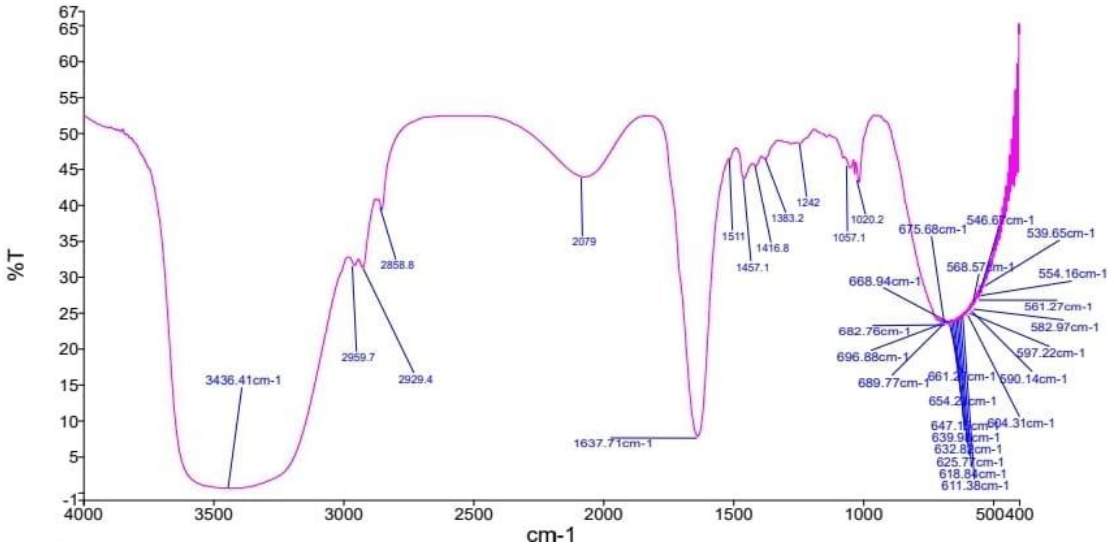

Fig. 4 : FTIR absorption spectrum obtained from copper nanoparticles.

4.5 FORMATION OF NANOPARTICLES :

Copper nanoparticles from ***Wild carrot*** were produced using 50 mL of a Copper sulphate pentahydarte solution (5 mM) and 5 mL of an aqueous plant extract. To lower the pH of the mixture to 7.0, NaOH (1 N) solution was added. Additionally, a green colour combination was created. After the mixture was centrifuged, pellets were collected, and they were overnight dried at 60°C in a hot air oven. The dark green powder was maintained at room temperature until it was needed (Kumar et al., 2025).

4.6 Phytochemical compounds identified by GC-MS analysis:

The GC-MS analysis of the data revealed the molecular formula, molecular weight, retention time, and peak area% of the active principles of the bioactive components of *Daucas Carota Linn*. The primary chemical components responsible for their anticancer activities include phytol, Hexadecanoic acid-methyl ester, n-Hexadecanoic- acid, Phytyl stearate, Octadecanoic acid

Table 2: Phytochemicals Identified by GC MS Analysis of *Daucas Carota Linn.*

S.No.	COMPOUND	MOLECULAR FORMULA	MOLECULAR WEIGHT	RETENTION TIME	AREA %	PEAK
1	Naphthalene, 1,2-dihydro-1,1,6 trimethy	$C_{13}H_{16}$	172	18.743	0.19	157
2	DL-Proline,5-oxo-,ethyl ester	$C_7H_{11}NO_3$	157	21.702	0.23	84
3	Phenol, 4-(3-methyl-2 buteny)	$C_{11}H_{14}O$	162	22.265	0.17	147
4	Decanoyl Chloride	$C_{10}H_{19}ClO$	190	23.171	0.59	55
5	Beta Carotene	$C_{40}H_{56}$	536	50.981	0.34	69

6	Lathosterol	$C_{27}H_{46}O$	386	53.999	0.28	255
7	Diosgnine	$C_{27}H_{42}O_3$	414	54.922	1.16	139
8	**Phytyl stearate**	**$C_{38}H_{74}O_2$**	**562**	**55.557**	**0.14**	**57**
9	Hydroxy-Beta-damascone	$C_{13}H_{20}O_2$	208	25.659	0.06	69
10	Longifolene	$C_{15}H_{24}$	204	26.798	0.22	161
11	8-pentadecanone	$C_{15}H_{30}O$	226	26.962	0.07	57
12	Cinnamic acid, 4-hydroxy-3-methoxy	$C_{31}H_{40}O_{15}$	652	27.857	0.34	105
13	1-hexadecanol	$C_{16}H_{34}O$	242	29.732	0.17	55
14	2-pentadecanone,6,10,14-trimethyl	$C_{18}H_{36}O$	268	30.826	0.59	58
15	1H-2-benzopyran-1-one,3,4-dihydro-8	$C_{11}H_{12}O_4$	208	30.893	0.73	164
16	2-cyclohexan-1-one,3-(3-hydroxybutyl	$C_{13}H_{22}O_2$	210	31.003	0.10	109
17	10-Nanodecanone	$C_{19}H_{38}O$	282	31.503	0.07	155
18	**Hexadecanoic acid, methyl ester**	**$C_{17}H_{34}O_2$**	**270**	**32.580**	**0.24**	**74**
19	9,12,15-octadecatrienoic acid,(Z,Z,Z)-	$C_{18}H_{30}O_2$	278	33.248	4.73	79
20	**n-Hexadecanoic- acid**	**$C_{16}H_{32}O_2$**	**256**	**33.248**	**12.85**	**73**
21	9,12-octadecadienoic acid (Z,Z)-methyl	$C_{19}H_{34}O_2$	294	35.958	0.25	67
22	9,12,15-octadecatrienoic acid, methyl	$C_{21}H_{26}O_2$	292	36.081	0.41	79

23	**Phytol**	**$C_{20}H_{40}O$**	**295**	**36.395**	**8.61**	**71**
24	9,12,15- octadecadienoic acid (Z,Z,Z)	$C_{18}H_{30}O_2$	278	37.373	17.34	
25	**Octadecanoic acid**	**$C_{18}H_{36}O_2$**	**284**	**37.672**	**0.37**	**73**
26	2-butenoicacid,2-methyl-,2-(acetyloxy-	$C_{27}H_{38}O_8$	490	39.655	0.87	
29	Octacosanol	$C_{28}H_{58}O$	410	43.135	0.51	55
30	Cyclohexane, bromo	$C_6H_{11}Br$	162	43.616	1.09	83
31	Cyclohexane, bromo	$C_6H_{11}Br$	162	43.720	1.24	83
32	1-hexacosanol	$C_{26}H_{54}O$	382	46.343	0.44	97
33	Octacosanol	$C_{28}H_{58}O$	410	49.435	0.26	55
34	Diosgnine	$C_{27}H_{42}O_3$	414	51.645	0.47	139
35	Dl-alpha-tocopherol	$C_{29}H_{50}O_2$	430	52.504	0.55	430
36	**Phytyl stearate**	**$C_{38}H_{74}O_2$**	**562**	**52.730**	**0.27**	**57**

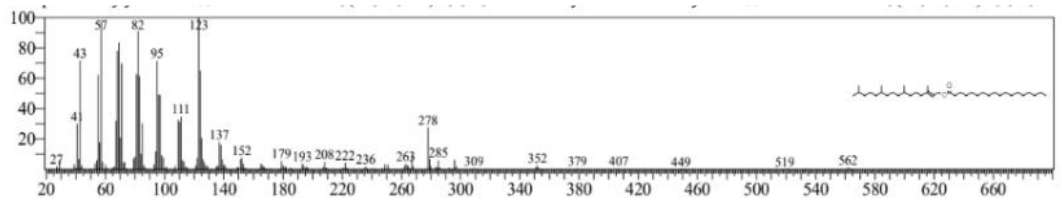

Compound:1

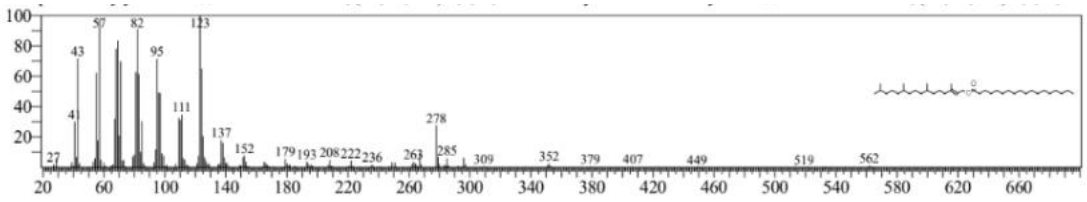

Compound: 2

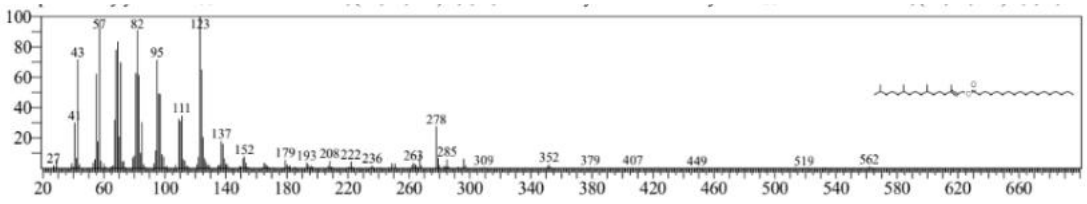

Compound: 3

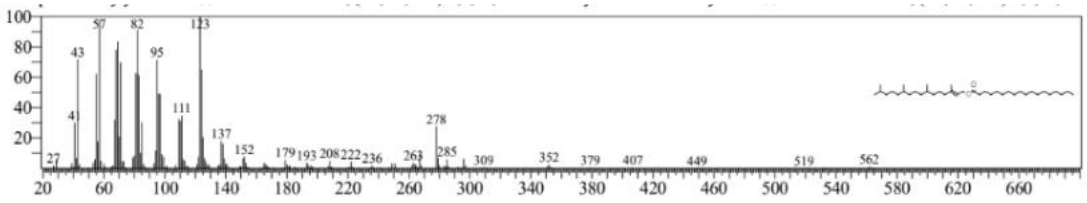

Compound: 4

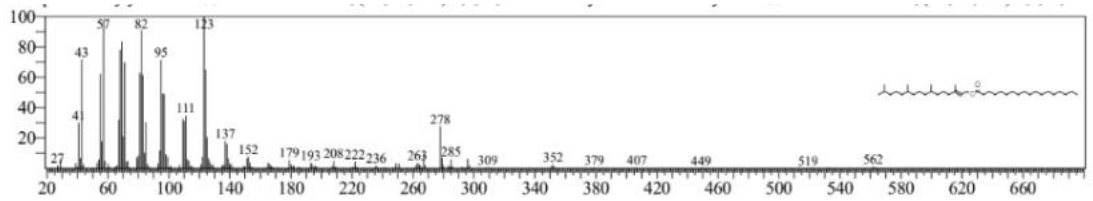

Compound: 5

4.7 Anticancer activity:

The Hep G-2 cancer cell line was utilized to test the anticancer effectiveness of plant extract and produced copper nanoparticles using the SBR assay. As compare to standard drug (Adriamycin), which had a GI50 value of <10 µg/mL, the Wild carrot leaves extract and copper nanoparticles, which had GI50 values of >80 µg/mL and >80 µg/mL, respectively, on the Hep G-2 cancer cell line, indicated % inhibition (Pei et al., 2023; Vijayakumar et al., 2021). The results are displayed in table 2:

Hep-G2	LC50	TGI	GI50*
A1	NE	NE	>80
A2	NE	NE	>80
ADR	16.6	<10	<10

Table 3: Anticancer potential of Plant extract, copper nanoparticles and Standard Drug: Drug concentrations (µg/ml) calculated from graph

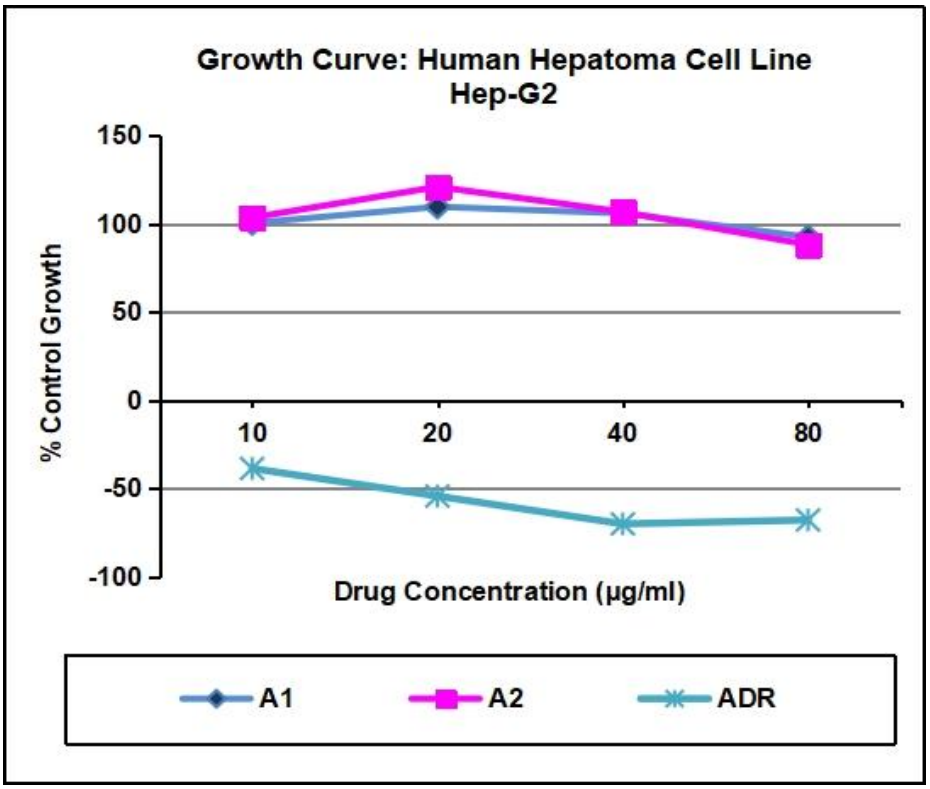

5. CONCLUSION

In this thesis, the extraction of Wild carrot leaves was used to prepare the formulation of copper nanoparticles. By turning dark green, copper nanoparticle synthesis may be verified. SEM, XRD, and FTIR were some of the techniques used to characterise nanoparticles. Spherical nanoparticles with a size range of 200 nm were present. XRD analysis verified the crystalline nature and face-cantered cubic structure. In the FTIR investigation, various functional groups were confirmed. SBR assay was used to evaluate the effectiveness of the anticancer With GI50 values of >80µg/ml, >80µg/ml, and 10µg/ml for plant extract, copper nanoparticles, as campare to standard drug (Adriamycin), respectively, anticancer potential was assessed using the SBR assay.

CONFLICT OF INTEREST

There is no conflict of interest

REFERENCES

[1] Das PE, Abu-Yousef IA, Majdalawieh AF, Narasimhan S, Poltronieri P. Green synthesis of encapsulated copper nanoparticles using a hydroalcoholic extract of Moringa oleifera leaves and assessment of their antioxidant and antimicrobial activities. Molecules. 2020 Jan 28;25(3):555.

[2] Dashtizadeh Z, Kashi FJ, Ashrafi M. Phytosynthesis of copper nanoparticles using Prunus mahaleb L. and its biological activity. Materials Today Communications. 2021 Jun 1;27:102456.

[3] Debela DT, Muzazu SG, Heraro KD, Ndalama MT, Mesele BW, Haile DC, Kitui SK, Manyazewal T. New approaches and procedures for cancer treatment: Current perspectives. SAGE open medicine. 2021 Aug;9:20503121211034366.

[4] Devi RS, Jeevitha M, Preetha S, Rajeshkumar S. Free radical scavenging activity of copper nanoparticles synthesized from dried ginger. Journal of Pharmaceutical Research International. 2020;32:1-7.

[5] Kumar D, Gupta, V, Tanwar, R. et al. From skin to bone: sun avoidance and osteoarthritis risk. Rheumatol Int 45, 146 (2025). https://doi.org/10.1007/s00296-025-05904-5

[6] Kumari P, Khatkar A, Rani P, Khatkar S, Nandal R. Optimizing the Microwave-Assisted Extraction Method to Enhance Extraction Yield and Total Phenolic Content from Moringa Leaves (Moringa oleifera Lam.). Cuestiones de Fisioterapia. 2024 Dec 3;53(03):464-82.

[7] Kumari P, Nandal R, Rani P, Rathi P, Khatkar S, Khatkar A. In Silico Screening of Phytoconstituents and Medicinal Plants as Antidiabetic Drug Discovery. Corrosion Management ISSN: 1355-5243. 2024;34(2):227-45.

[8] Liu H, Wang G, Liu J, Nan K, Zhang J, Guo L, Liu Y. Green synthesis of copper nanoparticles using Cinnamomum zelanicum extract and its applications as a highly efficient antioxidant and anti-human lung carcinoma. Journal of Experimental Nanoscience. 2021 Dec 15;16(1):410-23.

[9] Mali SC, Dhaka A, Githala CK, Trivedi R. Green synthesis of copper nanoparticles using Celastrus paniculatus Willd. leaf extract and their photocatalytic and antifungal properties. Biotechnology Reports. 2020 Sep 1;27:e00518.

[10] Pei J, Fu B, Jiang L, Sun T. Biosynthesis, characterization, and anticancer effect of plant-mediated silver nanoparticles using Coptis chinensis. International Journal of Nanomedicine. 2019 Mar 15:1969-78.

[11] Rani P, Pahwa R, Verma V, Bhatia M. Preparation, characterization, and evaluation of ketoconazole-loaded pineapple cellulose green nanofiber gel. International journal of biological macromolecules. 2024 Mar 1;262:130221.

[12] Rani P, Verma V, Kumar S, Bhatia M. Isolation, characterization and evaluation of pineapple crown waste nanofiber gel entrapping ampicillin in topical bacterial infections. Iranian Polymer Journal. 2024 May;33(5):687-98.

[13] Sarkar S, Kotteeswaran V. Green synthesis of silver nanoparticles from aqueous leaf extract of Pomegranate (Punica granatum) and their anticancer activity on human cervical cancer cells. Advances in Natural Sciences: Nanoscience and Nanotechnology. 2018 Jun 6;9(2):025014.

[14] ShanmugaSundaram C, Sivakumar J, Kumar SS, Ramesh PL, Zin T, Rao UM. Antibacterial and anticancer potential of Brassica oleracea var acephala using biosynthesised copper nanoparticles. The Medical Journal of Malaysia. 2020 Nov;75(6):615.

[15] Tahvilian R, Zangeneh MM, Falahi H, Sadrjavadi K, Jalalvand AR, Zangeneh A. Green synthesis and chemical

characterization of copper nanoparticles using Allium saralicum leaves and assessment of their cytotoxicity, antioxidant, antimicrobial, and cutaneous wound healing properties. Applied organometallic chemistry. 2019 Nov;33(12):e5234.

[16] Valsalam S, Agastian P, Arasu MV, Al-Dhabi NA, Ghilan AK, Kaviyarasu K, Ravindran B, Chang SW, Arokiyaraj S. Rapid biosynthesis and characterization of silver nanoparticles from the leaf extract of Tropaeolum majus L. and its enhanced in-vitro antibacterial, antifungal, antioxidant and anticancer properties. Journal of Photochemistry and Photobiology B: Biology. 2019 Feb 1;191:65-74.

[17] Vanaja D, Kavitha S. A study on phytochemicals, antioxidant activity and ft-ir analysis of Rhapis excelsa (thunb.) A. Henry. Eur J Pharm Med Res. 2016;3(7):390-4.

[18] Verma M, Deep A, Nandal R, Shinmar P, Kaushik D. Novel drug delivery system for cancer management: A review. Current Cancer Therapy Reviews. 2016 Dec 1;12(4):253-72.

[19] Vijayakumar G, Kesavan H, Kannan A, Arulanandam D, Kim JH, Kim KJ, Song HJ, Kim HJ, Rangarajulu SK. Phytosynthesis of copper nanoparticles using extracts of spices and their antibacterial properties. Processes. 2021 Jul 30;9(8):1341